Chapter 5

Sagnac Interferometer: Theory & Background

5.1 Introduction to Sagnac Interferometers

5.1.1 Development of Sagnac Interferometers

Sagnac provided the first demonstration of the feasibility of an optical experiment capable of indicating the state of rotation of a frame of reference, by making measurements within that frame, [25, 26]. A schematic diagram of his interferometer is shown in Fig. 5.1(i) .

The fringe pattern recorded at the output of this interferometer is sensitive to any phase difference between the two counter-propagating beams. In the case that the whole interferometer is rotating in its plane, at an angular frequency, $\mathbf{\Omega}_{\mathrm{rot}}$, it is possible to follow a simple derivation to obtain the value of the phase shift, $\Delta\phi$.

Consider a circular interferometer of radius, r, Fig. 5.1(ii). The time taken for the two beams to complete one circuit of the interferometer, $t_{\pm}$ is given by,

$$t_{\pm} = \frac{2\pi r \pm r \ \Omega_{\mathrm{rot}} t_{\pm}}{\mathrm{v}} \ ,$$

(5.1)

where v is the speed of propagation around the Sagnac loop.
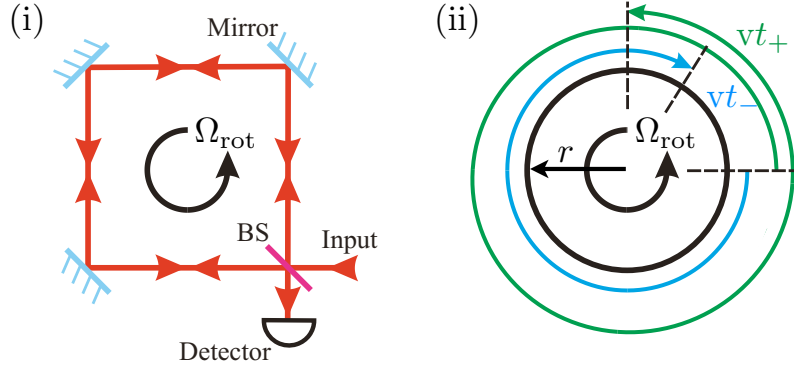
Figure 5.1: (i) A schematic diagram of Sagnac's original interferometer. Light from the light source is split into two beams by the beam splitter. Two counter-propagating beams then circulate the interferometer. The beams interfere on the beam splitter. There are two output ports of the interferometer, one back towards the light source, the other towards the detector. (ii) Shows a circular Sagnac interferometer of radius, r, rotating at an angular frequency, Ω_{rot}. The shifts in path length for the two counter-propagating beams, $\text{v}t_{\pm}$, are shown.

Thus,

$$t_{\pm} \left(\frac{\text{v} \mp r\,\Omega_{\text{rot}}}{\text{v}} \right) = \frac{2\pi r}{\text{v}} \ . \tag{5.2}$$

Hence

$$t_{\pm} = \frac{2\pi r}{\text{v} \mp r\,\Omega_{\text{rot}}} \ . \tag{5.3}$$

It follows that the difference in propagation time for the two counter-propagating beams, δt, is given by,

$$\delta t = t_{+} - t_{-} \ , \tag{5.4}$$

$$= \frac{2\pi r}{\text{v} - r\,\Omega_{\text{rot}}} - \frac{2\pi r}{\text{v} + r\,\Omega_{\text{rot}}} \ , \tag{5.5}$$

$$\implies \quad \delta t = \frac{4\pi r^2\,\Omega_{\text{rot}}}{\text{v}^2 - \left(r\,\Omega_{\text{rot}} \right)^2} \ . \tag{5.6}$$

The area of the interferometer, A, is equal to πr^2. The phase difference between the two counter-propagating beams, $\Delta\phi$, is given by $(\text{v}\,\delta t/\lambda_0)$.

In the vast majority of cases, $\text{v}^2 \gg \left(r\,\Omega_{\text{rot}} \right)^2$, it follows that,

$$\Delta\phi = \frac{4\boldsymbol{A} \cdot \boldsymbol{\Omega}_{\text{rot}}}{\lambda_0 \text{v}} \ . \tag{5.7}$$

Here $(\boldsymbol{A}/A)$ is a unit vector perpendicular to the surface area of the interferometer. In the case of light $v = c$, irrespective of a modified group velocity or phase velocity, [89].

The sensitivity of this interferometer due to rotations depends only on the wavelength, and the projection of the rotation onto the area enclosed within the interferometer. The centre of rotation and the shape of the loop have no bearing on the sensitivity. The sensitivity does however depend on the angle between the plane of rotation and the plane of the interferometer.

The Sagnac effect manifests itself in both Sagnac interferometers and Mach-Zehnder interferometers.

5.1.2   Types of Sagnac Interferometers

Since Sagnac's first measurements of rotation with his interferometer there has been a large amount of interest in making ever more sensitive measurements using a variety of different implementations of the Sagnac interferometer, [89, 90, 91].

There have been two main lines of development for Sagnac interferometers. Optical Sagnac interferometers, [89, 90, 91], aim to increase sensitivity by increasing the path length of the two beams before they are coupled out of the interferometer. There are two main schemes for achieving this, ring laser gyros and optical fibre gyros. Multiple loops around the same physical area lead to an increased gyroscopic area.

Matter-wave interferometers sensitive to the Sagnac effect are generally restricted to Mach-Zehnder interferometers, [92, 93, 94]. One notable exception is the Sagnac interferometer of Arnold *et al.*, [95]. Matter-wave interferometers have an intrinsic sensitivity much greater than optical Sagnac interferometers, due to the smaller velocity and wavelength of the particles compared to light. Matter-wave interferometers lose out to optical interferometers in that their enclosed area is limited. Where the sensitivity of optical-fibre interferometers is very easily scalable, for example by increasing the number of fibre loops, the sensitivity of matter-wave interferometers is not.

Optical ring laser gyros can achieve sensitivities of 1.4×10^{-11} rad s^{-1} Hz$^{-1/2}$,

[96], and atom interferometer gyroscopes can achieve sensitivities of 6×10^{-10} rad s^{-1} Hz$^{-1/2}$, [97].

5.1.3 Light-Matter-Wave Sagnac Interferometer

Zimmer and Fleischhauer, [17], have proposed a scheme that combines the scalability of optical Sagnac interferometers with the intrinsic greater sensitivity of matter-wave interferometers. The increased sensitivity comes from the slow-light phenomenon associated with EIT. Reducing the phase or group velocity of the light is not sufficient to enhance the Sagnac effect, [89]. If momentum is transferred from the slow light to a matter-wave, then this matter-wave component will lead to the enhancement of the Sagnac effect. It is likely that for this to be realized a low temperature atomic ensemble would be required, cooling to at least 10^3 T_{rec}[1].

5.1.4 Biased Sagnac

Measurements of the dispersion of the hyperfine structure of Cs were made using a Sagnac interferometer by Robins *et al.*, [99]. This required biasing the alignment of the interferometer, [100], such that the output arm contains two interference fringes. The difference signal between these two fringes gives a signal proportional to the dispersion of the medium.

This method was developed by Jundt *et al.*, [101], and applied to Rb hyperfine spectra. Rather than taking the difference between two fringes within one arm of the interferometer, the difference between two output arms of the interferometer was measured. This was shown to be in excellent agreement with the dispersion predicted from the transmission spectra using the Kramers-Kronig relations, § 2.3.2 on page 22 .

Furthermore, Purves *et al.*, [100], have applied the biased Sagnac interferometer to measuring EIT resonances. The basis for this publication is presented in chapter 6 of this thesis.

The theoretical basis showing that the difference signal between the two output

---

[1]$T_{\text{rec}} = (\hbar k_{\text{ab}})^2/(2m\text{k}_{\text{B}})$, [98], is the recoil temperature which for ^{87}Rb is 180 nK.

arms of the interferometer, in the case of biased alignment, is proportional to the dispersion is developed in § 5.3 on page 115 .

The biased Sagnac interferometer as described in § 5.3 on page 115 , provides a direct readout of the dispersion of a medium. The dispersion associated with a narrow EIT feature provides an ideal error signal which could be used to detect any physical effect that causes a shift in the detuning of the EIT resonance. For the purpose of making a detector, measuring the dispersion is more appropriate than simply measuring the absorption of the medium for two reasons: about line centre the rate of change in absorption with detuning is at a minimum, where as the rate of change in dispersion is at its maximum; secondly, also about line centre, the change in the absorption has the same sign independent of the sign of the shift in detuning, whereas the sign of the shift in dispersion is dependent upon the sign of the shift in detuning.

Mach-Zehnder interferometers have been used to measure the dispersion of a medium, [102], and specifically to measure the dispersion due to EIT, [3, 57]. There are two main advantages in using a Sagnac interferometer over a Mach-Zehnder: the stability of the interferometer against vibration and the control of the absolute difference in the length of the arms of the interferometer. The very nature of the Sagnac interferometer ensures that the default is to have no difference in path length between the two arms (the arms counter-propagate around the same loop). In addition to this the fact that both arms in the Sagnac interferometer interact with the same optical elements ensures a degree of common mode rejection in any vibrations that the optical elements experience.

It is of course possible to measure an error signal similar to that provided by the dispersion of a medium, by dithering the frequency of a probe beam while measuring the transmission. This has the added disadvantage of the dithering broadening the resonance, as well as requiring lock-in amplifiers to measure the error signal — these are complications not present with the biased Sagnac interferometer.

Measuring EIT in a Sagnac interferometer also paves the way for the realization of the optical-matter-wave interferometer of Zimmer and Fleischhauer, [17].

5.2 Beam Splitters

Following in the style of the analysis presented in *The Quantum Theory of Light*, by Loudon, [103], consider a beam splitter that does not have any losses. If we have two input fields, E_1 and E_2 and two output fields, E_3 and E_4, as in the diagram below, Fig. 5.2, it follows that the fields will be related by the following

E_3

E_1

E_4

Beam Splitter

E_2
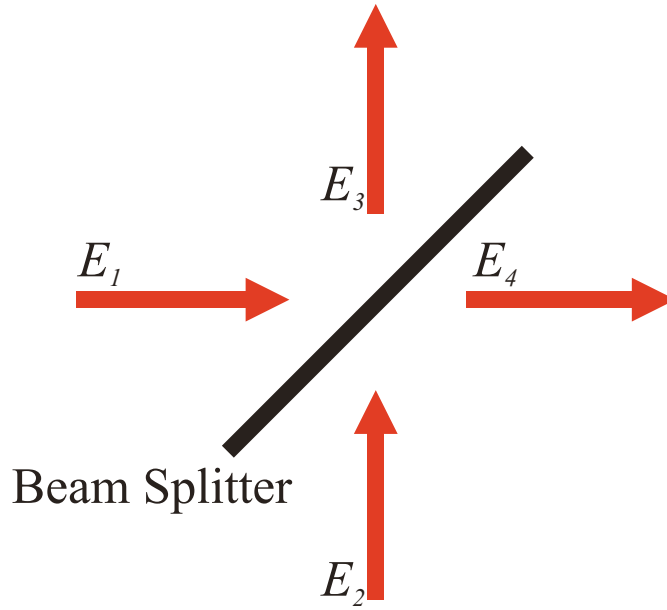
Figure 5.2: Two fields, E_1 and E_2, incident on the beam splitter lead to two output fields, E_3 and E_4.

equations,

$$E_3 = R_{31}E_1 + T_{32}E_2 , \qquad (5.8)$$

$$E_4 = T_{41}E_1 + R_{42}E_2 . \qquad (5.9)$$

Here R represents reflection and T represents transmission. R and T are both generally complex and vary with optical frequency. We will assume that we are dealing with monochromatic radiation. Equations 5.8 and 5.9 can be rewritten in matrix form as:

$$\begin{pmatrix} E_3 \\ E_4 \end{pmatrix} = \begin{pmatrix} R_{31} & T_{32} \\ T_{41} & R_{42} \end{pmatrix} \begin{pmatrix} E_1 \\ E_2 \end{pmatrix} . \qquad (5.10)$$

From the conservation of energy it follows that:

$$|E_3|^2 + |E_4|^2 \;=\; |E_1|^2 + |E_2|^2 \;, \tag{5.11}$$

$$= \; |R_{31}|^2|E_1|^2 + |T_{32}|^2|E_2|^2 + R_{31}T_{32}^*E_1E_2^*$$
$$+ R_{31}^*T_{32}E_1^*E_2 + |T_{41}|^2|E_1|^2 + |R_{42}|^2|E_2|^2 \tag{5.12}$$
$$+ T_{41}R_{42}^*E_1E_2^* + T_{41}^*R_{42}E_1^*E_2 \;.$$

From equation 5.12 ,

$$|R_{31}|^2 + |T_{41}|^2 \;=\; 1 \;,$$

$$= \; |T_{32}|^2 + |R_{42}|^2 \;, \tag{5.13}$$

$$R_{31}T_{32}^* + T_{41}R_{42}^* \;=\; 0 \;, \tag{5.14}$$

$$\text{or equivalently} \quad R_{31}^*T_{32} + T_{41}^*R_{42} \;=\; 0 \;. \tag{5.15}$$

The reflection and transmission coefficients can be written,

$$R_{31} \;=\; |R_{31}|\mathrm{e}^{\mathrm{i}\phi_{31}} \;, \tag{5.16}$$

$$R_{42} \;=\; |R_{42}|\mathrm{e}^{\mathrm{i}\phi_{42}} \;,$$

$$T_{32} \;=\; |T_{32}|\mathrm{e}^{\mathrm{i}\phi_{32}} \;,$$

$$T_{41} \;=\; |T_{41}|\mathrm{e}^{\mathrm{i}\phi_{41}} \;.$$

Substituting from equations 5.16 into equation 5.14, gives,

$$|R_{31}|\mathrm{e}^{\mathrm{i}\phi_{31}}|T_{32}|\mathrm{e}^{-\mathrm{i}\phi_{32}} + |T_{41}|\mathrm{e}^{\mathrm{i}\phi_{41}}|R_{42}|\mathrm{e}^{-\mathrm{i}\phi_{42}} \;=\; 0 \;,$$

$$\therefore \quad |R_{31}||T_{32}|\mathrm{e}^{\mathrm{i}(\phi_{31}-\phi_{32})} \;=\; -|R_{42}||T_{41}|\mathrm{e}^{\mathrm{i}(\phi_{41}-\phi_{42})} \;,$$

$$\therefore \quad |R_{31}||T_{32}|\mathrm{e}^{\mathrm{i}(\phi_{31}+\phi_{42}-\phi_{32}-\phi_{41})} \;=\; -|R_{42}||T_{41}| \;. \tag{5.17}$$

Equating the imaginary parts of equation 5.17,

$$|R_{31}||T_{32}|\sin\left(\phi_{31} + \phi_{42} - \phi_{32} - \phi_{41}\right) \;=\; 0 \;,$$

$$\implies \phi_{31} + \phi_{42} - \phi_{32} - \phi_{41} \;=\; -\pi, 0, +\pi \;. \tag{5.18}$$

It follows that,

$$\cos\left(\phi_{31} + \phi_{42} - \phi_{32} - \phi_{41}\right) = \pm 1 \;. \tag{5.19}$$

Equating real parts of equation 5.17,

$$|R_{31}||T_{32}| > 0 ,$$
$$|R_{42}||T_{41}| > 0 ,$$
$$\text{hence} \quad \cos(\phi_{31} + \phi_{42} - \phi_{32} - \phi_{41}) < 0 .$$

Thus from equation 5.19 ,

$$\cos(\phi_{31} + \phi_{42} - \phi_{32} - \phi_{41}) = -1 , \tag{5.20}$$
$$\implies \quad \phi_{31} + \phi_{42} - \phi_{32} - \phi_{41} = \pm\pi , \tag{5.21}$$

It follows that,

$$\frac{|R_{31}|}{|T_{41}|} = \frac{|R_{42}|}{|T_{32}|} . \tag{5.22}$$

Hence the ratios into which the radiation is split is the same whether it comes in from side "1" or side "2". Thus from equations 5.13 and 5.22,

$$|R_{31}| = |R_{42}| ,$$
$$\equiv |R| , \tag{5.23}$$

$$\text{and} \quad |T_{31}| = |T_{42}| ,$$
$$\equiv |T| . \tag{5.24}$$

Taking the beam splitter coefficients to be symmetrical,

$$\phi_{31} = \phi_{42} ,$$
$$\equiv \phi_{\mathrm{R}} , \tag{5.25}$$

$$\text{and} \quad \phi_{32} = \phi_{41} ,$$
$$\equiv \phi_{\mathrm{T}} . \tag{5.26}$$

It follows from equations 5.25, 5.26 and 5.21 that,

$$\phi_{\mathrm{R}} - \phi_{\mathrm{T}} = \pm\frac{\pi}{2} . \tag{5.27}$$

Hence,

$$R_{31} = R_{42} \ ,$$
$$= R \ ,$$
$$R = |R|\mathrm{e}^{\mathrm{i}\phi_\mathrm{R}} \ , \tag{5.28}$$

$$T_{32} = T_{41} \ ,$$
$$= T \ ,$$
$$T = |T|\mathrm{e}^{\mathrm{i}\phi_\mathrm{T}} \ . \tag{5.29}$$

Thus the transmission and reflection is the same, independent of which side of the beam splitter the beam is input from.

5.3 Sagnac Interferometer

The Sagnac interferometer used to make measurements of EIT features in chapter 6 is shown in Fig. 5.3 on the following page .

Consider four different paths of the probe beam around the Sagnac interferometer to one of the photodiodes, Fig. 5.4. The beam can propagate around the photodiode in one of two directions: clockwise, which will be labelled with the subscript "c"; and anticlockwise which will be labelled "a". Both the clockwise and anticlockwise beams will have components that will impinge on each of the photodiodes. The two photodiodes are labelled "A" and "B", and those subscripts will be used to label the components in the derivation. Fig. 5.4 on page 117 shows the four possible paths around the interferometer. To determine the intensity of light measured at each photodiode it is necessary to first find the amplitude of each component that arrives at that photodiode, and then take the magnitude of the field squared. It will be necessary to consider the phase and amplitude modifications of each field around the interferometer. As each field is derived from the same probe beam, then only the changes to the fields once they are split into the two oppositely propagating fields needs to be considered. For the purpose of this derivation, assume that the beam splitters and mirrors are lossless. Also assume that any phase picked up on the mirrors is the same for both beams.
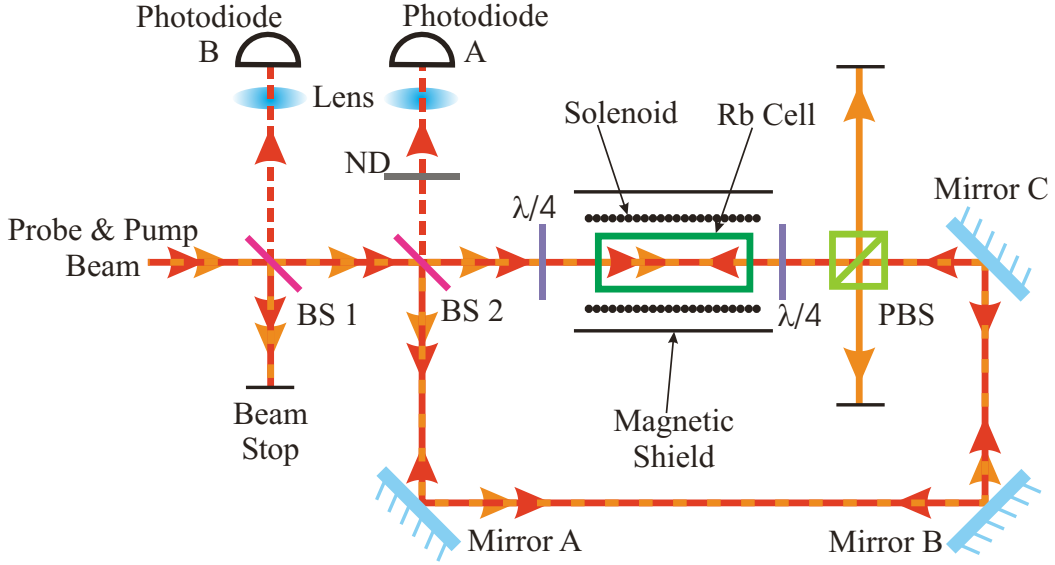
Figure 5.3: BS1 and BS2 are the first and second 50:50 beam splitters respectively; ND is the neutral-density filter; PBS is the polarizing beam splitter and $\lambda/4$ is a quarter-wave plate. The probe beams are drawn in red and the pump beams in orange. The Sagnac interferometer is formed by the loop originating and terminating at the second beam splitter (BS2). Output arm A propagates towards photodiode A and output arm B towards photodiode B.

It will also be instructive to consider a small misalignment between the two beams. This will be done by assuming a small path difference of length Δl between the clockwise and the anticlockwise propagating beams. Both beams pick up the same phase shift due to passing through the first beam splitter. This phase is therefore neglected in the following analysis.

$$\frac{E_{\text{A, c}}}{E_{\text{Input}}} = |T_1||T_{\text{ND}}|\left[e^{-\frac{\alpha_c L}{2}}e^{i(kn_c L+2\phi_{2\text{T}}+\phi_{\text{ND}})}|T_2|^2\right], \tag{5.30}$$

$$\frac{E_{\text{A, a}}}{E_{\text{Input}}} = |T_1||T_{\text{ND}}|\left[e^{-\frac{\alpha_a L}{2}}e^{i(k(n_a L+\Delta l)+2\phi_{2\text{R}}+\phi_{\text{ND}})}|R_2|^2\right], \tag{5.31}$$

$$\frac{E_{\text{B, c}}}{E_{\text{Input}}} = |T_1||R_1|\left[e^{-\frac{\alpha_c L}{2}}e^{i(kn_c L+\phi_{2\text{T}}+\phi_{2\text{R}}+\phi_{1\text{R}})}|T_2||R_2|\right], \tag{5.32}$$

$$\frac{E_{\text{B, a}}}{E_{\text{Input}}} = |T_1||R_1|\left[e^{-\frac{\alpha_a L}{2}}e^{i(k(n_a L+\Delta l)+\phi_{2\text{R}}+\phi_{2\text{T}}+\phi_{1\text{R}})}|T_2||R_2|\right]. \tag{5.33}$$

To determine the normalized intensity of the fields at both photodiodes sum
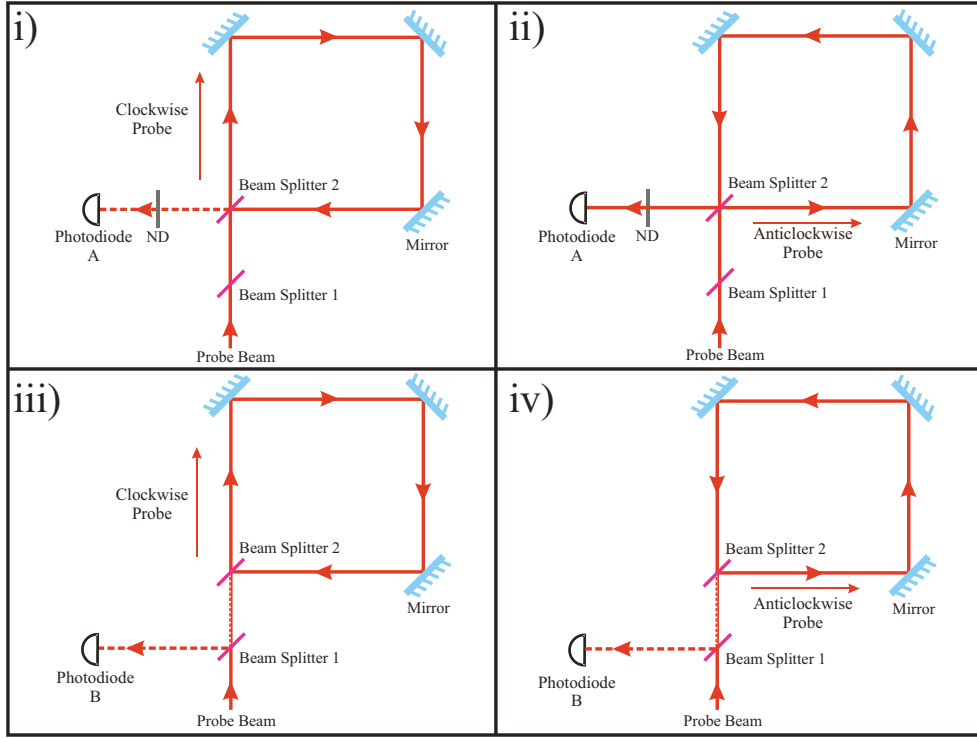
Figure 5.4: (i) and (ii) show the path of the clockwise and anticlockwise propagating beam to photodiode A. (iii) and (iv) show the path of the clockwise and anticlockwise propagating beam to photodiode B. ND is a neutral density filter.

the amplitudes of the fields at each photodiode and then multiply them by the complex conjugate to obtain the modulus squared.

$$I_A = \left| \frac{E_{A,\,c} + E_{A,\,a}}{E_{\text{Input}}} \right|^2, \tag{5.34}$$

$$I_B = \left| \frac{E_{B,\,c} + E_{B,\,a}}{E_{\text{Input}}} \right|^2. \tag{5.35}$$

$$
\begin{aligned}
I_A &= \left(|T_1||T_{\text{ND}}|\right)^2 \left[e^{-\frac{\alpha_c L}{2}} e^{i(kn_c L + 2\phi_{2T})} |T_2|^2 + e^{-\frac{\alpha_a L}{2}} e^{i(k(n_a L + \Delta l) + 2\phi_{2R})} |R_2|^2 \right] \\
&\quad \times \left[e^{-\frac{\alpha_c L}{2}} e^{-i(kn_c L + 2\phi_{2T})} |T_2|^2 + e^{-\frac{\alpha_a L}{2}} e^{-i(k(n_a L + \Delta l) + 2\phi_{2R})} |R_2|^2 \right], \tag{5.36}
\end{aligned}
$$

$$
\begin{aligned}
&= |T_1|^2 |T_{\text{ND}}|^2 \left[|T_2|^4 e^{-\alpha_c L} + |R_2|^4 e^{-\alpha_a L} + |T_2|^2 |R_2|^2 e^{-(\alpha_c + \alpha_a)\frac{L}{2}} \right. \tag{5.37} \\
&\quad \left. \times \left(e^{i(kn_c L + 2\phi_{2T}) - i(k(n_a L + \Delta l) + 2\phi_{2R})} + e^{i(k(n_a L + \Delta l) + 2\phi_{2R}) - i(kn_c L + 2\phi_{2T})} \right) \right].
\end{aligned}
$$

Now writing,

$$\alpha = \frac{\alpha_c + \alpha_a}{2} \,,$$

$$\Delta n = n_c - n_a \,,$$

and also from equation 5.27, $(\phi_R - \phi_T = -\pi/2)$, we can rewrite the intensity at photodiode A as,

$$
\begin{aligned}
I_A &= |T_1|^2 |T_{ND}|^2 \left[|T_2|^4 e^{-\alpha_c L} + |R_2|^4 e^{-\alpha_a L} \right. \tag{5.38} \\
&\quad \left. + |T_2|^2 |R_2|^2 e^{-\alpha L} \left(e^{ikL\Delta n - \Delta l + i\pi} + e^{-ik(L\Delta n + \Delta l) - i\pi} \right) \right] \,,
\end{aligned}
$$

$$
\begin{aligned}
&= |T_1|^2 |T_{ND}|^2 \left[|T_2|^4 e^{-\alpha_c L} + |R_2|^4 e^{-\alpha_a L} \right. \\
&\quad \left. - |T_2|^2 |R_2|^2 e^{-\alpha L} 2 \cos \left(k \left(L\Delta n - \Delta l \right) \right) \right] \,,
\end{aligned}
$$

$$
\begin{aligned}
\therefore \quad I_A &= |T_1|^2 |T_{ND}|^2 \left[|T_2|^4 e^{-\alpha_c L} + |R_2|^4 e^{-\alpha_a L} \right. \\
&\quad \left. - 2|T_2|^2 |R_2|^2 e^{-\alpha L} \cos \left(k \left(L\Delta n - \Delta l \right) \right) \right] \,. \tag{5.39}
\end{aligned}
$$

Considering the other output arm of the Sagnac interferometer,

$$
\begin{aligned}
I_B &= (|T_1||R_1|)^2 \left[e^{-\frac{\alpha_c L}{2}} e^{i(kn_c L + \phi_{2T} + \phi_{2R} + \phi_{1R})} |T_2||R_2| \right. \\
&\quad \left. + e^{-\frac{\alpha_a L}{2}} e^{i(k(n_a L + \Delta l) + \phi_{2R} + \phi_{2T} + \phi_{1R})} |R_2||T_2| \right] \\
&\quad \times \left[e^{-\frac{\alpha_c L}{2}} e^{-i(kn_c L + \phi_{2T} + \phi_{2R} + \phi_{1R})} |T_2||R_2| \right. \\
&\quad \left. + e^{-\frac{\alpha_a L}{2}} e^{-i(k(n_a L + \Delta l) + \phi_{2R} + \phi_{2T} + \phi_{1R})} |R_2||T_2| \right] \,. \tag{5.40}
\end{aligned}
$$

As with the derivation above for I_A, rewriting the equation for I_B in terms of Δn and α, then we get

$$
\begin{aligned}
I_B &= |T_1|^2 |R_1|^2 \left[|R_2|^2 |T_2|^2 e^{-\alpha_c L} + |R_2|^2 |T_2|^2 e^{-\alpha_a L} \right. \tag{5.41} \\
&\quad \left. + |T_2|^2 |R_2|^2 e^{-\alpha L} \left(e^{ik(L\Delta n - \Delta l)} + e^{-ik(L\Delta n + \Delta l)} \right) \right] \,,
\end{aligned}
$$

$$
\begin{aligned}
&= |T_1|^2 |R_1|^2 \left[|R_2|^2 |T_2|^2 e^{-\alpha_c L} + |R_2|^2 |T_2|^2 e^{-\alpha_a L} \right. \\
&\quad \left. + 2|T_2|^2 |R_2|^2 e^{-\alpha L} \cos \left(k \left(L\Delta n - \Delta l \right) \right) \right] \,,
\end{aligned}
$$

$$
\begin{aligned}
\therefore \quad I_B &= |T_1|^2 |R_1|^2 |T_2|^2 |R_2|^2 \left[e^{-\alpha_c L} + e^{-\alpha_a L} \right. \\
&\quad \left. + 2 e^{-\alpha L} \cos \left(k \left(L\Delta n - \Delta l \right) \right) \right] \,. \tag{5.42}
\end{aligned}
$$

From equations 5.39 and 5.42 the sum and the difference signals can be derived,

$$
\begin{aligned}
I_A + I_B &= e^{-\alpha_c L} \left(|T_1|^2 |T_{ND}|^2 |T_2|^4 + |T_1|^2 |R_1|^2 |T_2|^2 |R_2|^2 \right) \\
&\quad + e^{-\alpha_a L} \left(|T_1|^2 |T_{ND}|^2 |T_2|^4 + |T_1|^2 |R_1|^2 |T_2|^2 |R_2|^2 \right) \quad (5.43) \\
&\quad + e^{-\alpha L} \left(|T_1|^2 |R_1|^2 |T_2|^2 |R_2|^2 \right. \\
&\quad \left. - |T_1|^2 |T_{ND}|^2 |T_2|^2 |R_2|^2 \right) 2\cos\left(k\left(L\Delta n - \Delta l \right) \right),
\end{aligned}
$$

$$
\begin{aligned}
I_A - I_B &= e^{-\alpha_c L} \left(|T_1|^2 |T_{ND}|^2 |T_2|^4 - |T_1|^2 |R_1|^2 |T_2|^2 |R_2|^2 \right) \\
&\quad + e^{-\alpha_a L} \left(|T_1|^2 |T_{ND}|^2 |T_2|^4 - |T_1|^2 |R_1|^2 |T_2|^2 |R_2|^2 \right) \quad (5.44) \\
&\quad + e^{-\alpha L} \left(-|T_1|^2 |R_1|^2 |T_2|^2 |R_2|^2 \right. \\
&\quad \left. - |T_1|^2 |T_{ND}|^2 |T_2|^2 |R_2|^2 \right) 2\cos\left(k\left(L\Delta n - \Delta l \right) \right).
\end{aligned}
$$

Consider the particular case where the intensity of an incoming beam is split equally into two components each of which has 50 % of the incoming intensity. Also the ND filter will transmit only 50 % of the incident intensity.

Therefore,

$$
\begin{aligned}
|T_1| &= |T_2|, \\
&= |T_{ND}|, \\
&= |R_1|, \quad\quad\quad (5.45) \\
&= |R_2|, \\
&= \frac{1}{\sqrt{2}}.
\end{aligned}
$$

Then, from equations 5.43, 5.44 and 5.45,

$$
I_A + I_B = \frac{1}{8} \left(e^{-\alpha_c L} + e^{-\alpha_a L} \right), \quad\quad (5.46)
$$

$$
I_A - I_B = -\frac{1}{4} e^{-\alpha L} \cos\left(k\left(L\Delta n - \Delta l \right) \right). \quad\quad (5.47)
$$

In practice any misalignment of the Sagnac will lead to there being a range of Δl across the finite profile of the output beams. As the whole beam is generally focussed onto a photodiode then what will be recorded is an average over a range of Δl of I_A and I_B. In order to determine what is recorded, it is necessary to integrate I_A and I_B over a range of Δl. From equations 5.39 and 5.42 this

leads to,

$$
\begin{aligned}
\int_{\Delta l_1}^{\Delta l_2} I_{\mathrm{A}} \mathrm{d}\left(\Delta l\right) \;=\;& |T_1|^2 |T_{\mathrm{ND}}|^2 \left[\left(|T_2|^4 \mathrm{e}^{-\alpha_{\mathrm{c}} L} + |R_2|^4 \mathrm{e}^{-\alpha_{\mathrm{a}} L} \right) \Delta l \right. \\
& \left. -2|T_2|^2 |R_2|^2 \mathrm{e}^{-\alpha L} \left(\frac{1}{k} \right) \sin\left(k\left(L\Delta n - \Delta l \right) \right) \right]_{\Delta l_1}^{\Delta l_2} ,
\end{aligned}
\tag{5.48}
$$

$$
\begin{aligned}
\;=\;& |T_1|^2 |T_{\mathrm{ND}}|^2 \left[\left(|T_2|^4 \mathrm{e}^{-\alpha_{\mathrm{c}} L} + |R_2|^4 \mathrm{e}^{-\alpha_{\mathrm{a}} L} \right) \left(\Delta l_2 - \Delta l_1 \right) \right. \\
& -2|T_2|^2 |R_2|^2 \mathrm{e}^{-\alpha L} \left(\frac{1}{k} \right) \left[\sin\left(k\left(L\Delta n - \Delta l_2 \right) \right) \right. \\
& \left. \left. - \sin\left(k\left(L\Delta n - \Delta l_1 \right) \right) \right] \right] .
\end{aligned}
\tag{5.49}
$$

but,
$$
\sin\alpha - \sin\beta \;=\; 2\sin\left(\frac{\alpha - \beta}{2} \right) \cos\left(\frac{\alpha + \beta}{2} \right) ,
\tag{5.50}
$$

$$
\begin{aligned}
\implies \sin\left(k\left(L\Delta n - \Delta l_2 \right) \right) \;-\;& \sin\left(k\left(L\Delta n - \Delta l_1 \right) \right) \\
\;=\;& 2\sin\left(\frac{k\left(\Delta l_1 - \Delta l_2 \right)}{2} \right) \cos\left(kL\Delta n - \frac{k}{2}\left(\Delta l_2 + \Delta l_1 \right) \right) .
\end{aligned}
\tag{5.51}
$$

Using the fact that,

$$
\cos\left(\theta \pm \phi \right) \;=\; \cos\theta \cos\phi \mp \sin\theta \sin\phi ,
\tag{5.52}
$$

$$
\mathrm{for} \quad \phi \;=\; \frac{\pi}{2} ,
$$

$$
\mathrm{then,} \quad \cos\left(\theta - \frac{\pi}{2} \right) \;=\; \sin\theta .
\tag{5.53}
$$

To measure small changes in the refractive index directly, it is desirable to have sine terms as opposed to cosine terms, with an argument proportional to Δn, in the output of both arms of the Sagnac. In the limits of the arguments being small, sine terms can be approximated as being equal to the argument.

This requires,

$$
\frac{k}{2}\left(\Delta l_2 + \Delta l_1 \right) \;=\; \frac{\pi}{2} ,
\tag{5.54}
$$

$$
\mathrm{and\ if,} \quad k\Delta l_1 \;=\; 0 ,
\tag{5.55}
$$

$$
\mathrm{then,} \quad k\Delta l_2 \;=\; \pi .
\tag{5.56}
$$

Thus,

$$
\begin{aligned}
\sin\left(k\left(L\Delta n - \Delta l_2 \right) \right) \;-\;& \sin\left(k\left(L\Delta n - \Delta l_1 \right) \right) \\
&= 2\sin\left(-\frac{\pi}{2} \right) \sin\left(kL\Delta n \right), \\
&= -2\sin\left(kL\Delta n \right).
\end{aligned}
\tag{5.57}
$$

Substituting equation 5.57 into equation 5.49,

$$\int_{\Delta l_1}^{\Delta l_2} I_{\mathrm{A}} \mathrm{d}\left(\Delta l\right) = |T_1|^2 |T_{\mathrm{ND}}|^2 \left[\left(|T_2|^4 \mathrm{e}^{-\alpha_{\mathrm{c}}L} + |R_2|^4 \mathrm{e}^{-\alpha_{\mathrm{a}}L}\right)\left(\frac{\pi}{k}\right)\right.$$
$$\left. + \frac{4}{k}|T_2|^2 |R_2|^2 \mathrm{e}^{-\alpha L} \sin\left(kL\Delta n\right)\right] . \tag{5.58}$$

Similarly for I_{B},

$$\int_{\Delta l_1}^{\Delta l_2} I_{\mathrm{B}} \mathrm{d}\left(\Delta l\right) = |T_1|^2 |R_1|^2 |T_2|^2 |R_2|^2 \left[\left(\mathrm{e}^{-\alpha_{\mathrm{c}}L} + \mathrm{e}^{-\alpha_{\mathrm{a}}L}\right)\left(\frac{\pi}{k}\right)\right.$$
$$\left. - \frac{4}{k}\mathrm{e}^{-\alpha L} \sin\left(kL\Delta n\right)\right] . \tag{5.59}$$

Therefore the sum and difference signals are given by,

$$\int_{\Delta l_1}^{\Delta l_2} I_{\mathrm{A}} \mathrm{d}\left(\Delta l\right) + \int_{\Delta l_1}^{\Delta l_2} I_{\mathrm{B}} \mathrm{d}\left(\Delta l\right) = \frac{\pi}{8k}\left(\mathrm{e}^{-\alpha_{\mathrm{c}}L} + \mathrm{e}^{-\alpha_{\mathrm{a}}L}\right) , \tag{5.60}$$

$$\int_{\Delta l_1}^{\Delta l_2} I_{\mathrm{A}} \mathrm{d}\left(\Delta l\right) - \int_{\Delta l_1}^{\Delta l_2} I_{\mathrm{B}} \mathrm{d}\left(\Delta l\right) = \frac{\mathrm{e}^{-\alpha L}}{2k} \sin\left(kL\Delta n\right) , \tag{5.61}$$

in the case that equation 5.45 applies.

From equations 5.60 and 5.61, the sum, S_{S}, and difference, S_{D} signals can be determined,

$$S_{\mathrm{S}} \propto \mathrm{e}^{-\alpha_{\mathrm{c}}L} + \mathrm{e}^{-\alpha_{\mathrm{a}}L} , \tag{5.62}$$

$$S_{\mathrm{D}} \propto \mathrm{e}^{-\alpha L} \sin\left(kL\Delta n\right) . \tag{5.63}$$

Hence the sum signal is proportional to the sum of the transmission of the two counter-propagating probes. The difference signal is proportional to the sine of the difference in refractive index between the two directions of propagation. In the case that $kL\Delta n \ll 1$ it follows that,

$$S_{\mathrm{D}} \propto \mathrm{e}^{-\alpha L} kL\Delta n . \tag{5.64}$$

Thus for a Sagnac interferometer, as described in this chapter, comprising two 50:50 beam splitters, the difference signal between the two output ports will be proportional to the difference in the real part of the refractive index between the two counter-propagating arms.